❒   108

Cascaded H-bridge 7-level inverter application for air exhaust fan drive control of Thu Thiem road tunnel

An Thi Hoai Thu Anh[1], Tran Hung Cuong[2], Tran Van Khoi[1]

[1]Department of Electrical Engineering, Faculty of Electrical and Electronics Engineering, University of Transport and Communications, Hanoi, Vietnam
[2]Division of Electrical & Electronics Engineering, Faculty of Electrical and Electronic Engineering, Thuyloi University, Hanoi, Vietnam

Article Info

ABSTRACT

The Thu Thiem road tunnel in Vietnam is crucial in reducing traffic congestion and ensuring the safety of those passing through, thanks to its ventilation system that generates clean air. This fresh air production is primarily supported by two exhaust fans at both ends of the tunnel in the eastern and western towers. However, the fans have a power capacity of several hundred kW and operate at kilovolt-level voltage, which is unsuitable for conventional inverters. Therefore, this paper proposes a 7-level inverter to feed the exhaust fan drive motor. The 7-level inverter improves the output voltage quality, and the output current and voltage have reduced the harmonic distortion significantly. The outstanding advantages of this inverter are verified through MATLAB/Simulink simulation software compared to a 3-level inverter.

Corresponding Author:

Tran Hung Cuong
Division of Electrical & Electronics Engineering, Faculty of Electrical and Electronics Engineering
Thuyloi University
Hanoi, Vietnam
Email: cuongth@tlu.edu.vn

1. INTRODUCTION

The road tunnel not only contributes significantly to the economic and social development but also improves the quality of citizens' lives of each nation, easing traffic congestion by creating an alternative route for vehicles, especially in areas with high traffic density, increasing travel speed between destinations, reducing travel time, and enhancing the efficiency of the transportation system. However, road tunnels also face disadvantages because of the closed and long tunnels. With many vehicles in the tunnel, a significant amount of toxic gases such as NO, CO, CO_2, and SO_2 is released, which can seriously affect the health and safety of those using the tunnel [1], [2] and the amount of gas in the tunnel must be cleaned before being taken out [3], [4]. Thu Thiem road tunnel, the most advanced modern tunnel in Ho Chi Minh city, is designed to traverse the Saigon River. Inside the tunnel are six spacious lanes for two-way traffic, with lane widths ranging from 2 m to 3.5 m. The maximum speed for motorcycles is 40 km/h, while cars can travel at 60 km/h within the tunnel. The ventilation system shown in Figure 1 includes several devices: electrostatic precipitator (EP), 04 exhaust fans (TVF), 12 jet fans (JF), escape ventilation fans, and air quality measurement sensors. Among equipment, each exhaust fan motor is 525 kW and has a voltage of 6 kV. Therefore, multi-level inverters are suitable for feeding large power motors and are applied in industry, transportation, and renewable energy resources [5]-[11].

Multilevel inverters that can generate the output voltage with very harmonic distortion, lower than that of conventional inverters, increasing the duration of power semiconductor switches, are divided into

three types: neutral-point diode-clamped multilevel inverter (NPC), flying capacitor multilevel inverter, and cascaded H-bridge inverter (CHB) [12]-[16]. Table 1 shows that CHB uses the fewest components. In the three configurations in Table 1, CHBs use the fewest components. Additionally, each H-bridge cell operates at a lower voltage, reducing stress on the components and thereby improving the reliability and lifespan of the inverter. The CHB inverter can also be configured for many applications, including medium and high voltage applications, making it flexible for different power inverters [17]-[20]. The article's content focuses on 7-level inverters applied to exhaust fans, as shown in Figure 2.
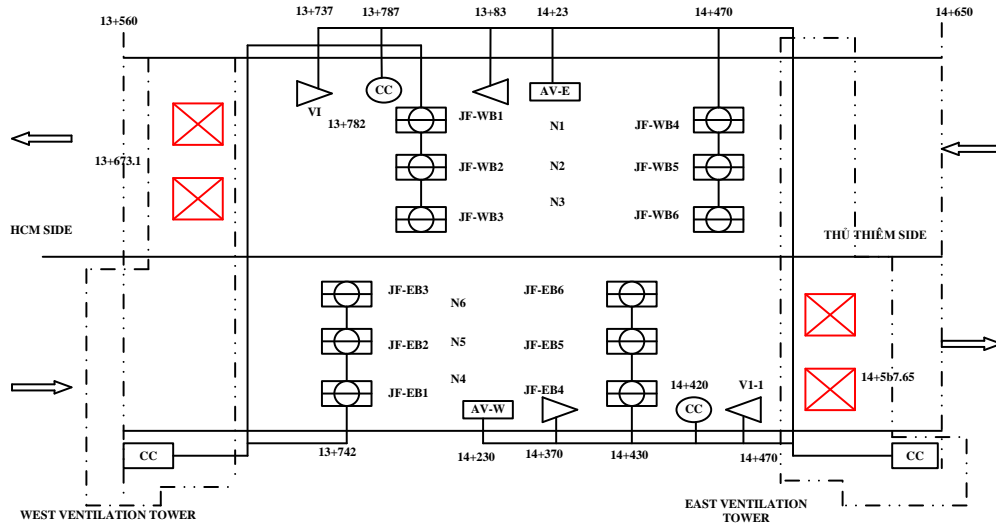

Figure 1. The four exhaust fans installed in the tunnel in red

Table 1. Comparison of the numbers of components in one phase of three types of inverters with n- n-levels

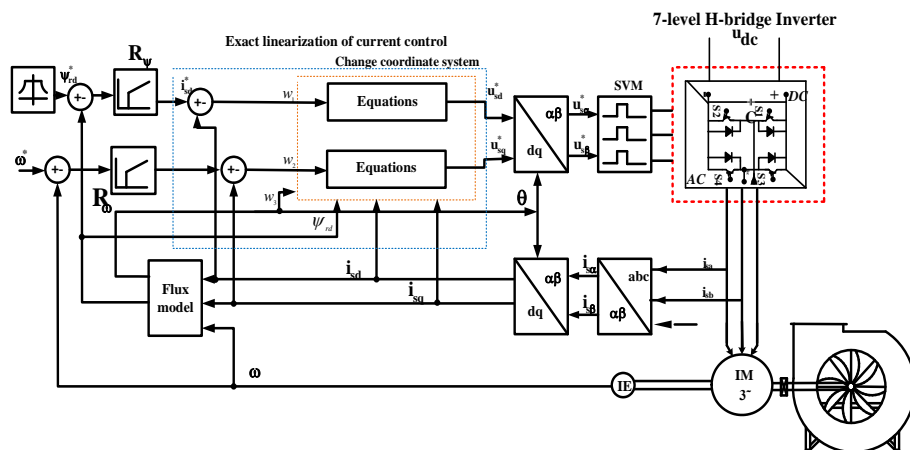| Topology of inverter	NPC	FC	CHB
IGBT	2(n-1)	2(n-1)	2(n-1)
Diode paralleled with IGBT	2(n-1)	2(n-1)	2(n-1)
Clamp diode	(n-1)(n-2)	0	0
Capacitors on DC source	(n-1)	(n-1)	(n-1)/2
Balancing capacitors	0	(n-1)(n-2)/2	0

Figure 2. The CHB 7-level inverter fed the exhaust fan drive system

2. DESIGN CONTROL FOR CASCADED H- BRIDGE 7-LEVEL INVERTER

Figure 2 shows the control structure of a CHB 7-level inverter with the field oriented control (FOC) method, including the current control loop using the exact linearization method, flux control, speed control loops with PI controllers [21]-[25] and 7-level voltage source inverter fed induction motor (IM) demonstrated in Figure 3 includes three single–phase topologies, the DC sources u_{dc} must be isolated from each other; each

AC output connected to output A, B, C of three-phase balanced loads $Z_a=Z_b=Z_c$, and a common terminal at point N is also an isolation point, Z is the neutral point of load.
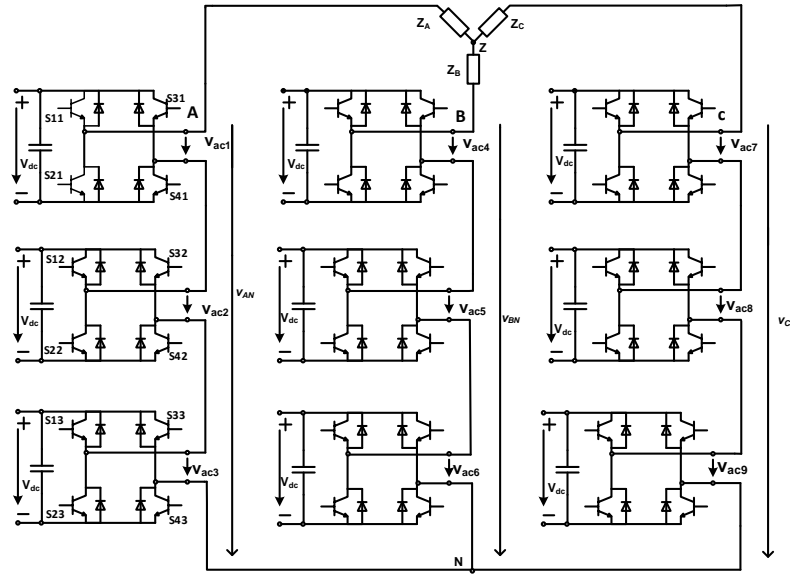

Figure 3. The three-phase structure of 7- level cascaded inverter

2.1. The space vector modulation of the 7-level voltage source inverter

The space vector modulation of the 7-level voltage source inverter is conducted in three steps:
Step 1: determine the state vector, voltage vector and corresponding voltage value

Assume that the three V_{DC} voltages are balanced and equal to each other. Output voltage on each phase V_{AN}, V_{BN}, V_{CN} can receive one of seven levels: $+/–Vdc$, 0, $+/-2Vdc$, $+/-3Vdc$. The voltage across each phase of the inverter load is equal to:

$$\begin{cases} v_{AN} = k_A.V_{DC} \\ v_{BN} = k_B.V_{DC} \\ v_{CN} = k_C.V_{DC} \end{cases} \text{With } (k_A, k_B, k_C)=\{3; 2; 1; 0; -1; -2; -3\} \tag{1}$$

Assuming the three phases are load balanced, the voltage across each phase of the load will be equal to:

$$\begin{cases} v_A = v_{AN} - v_{ZN} \\ v_B = v_{BN} - v_{ZN} \\ v_C = v_{CN} - v_{ZN} \end{cases} \text{with } v_A+v_B+v_C=0; \ v_{ZN} = \frac{1}{3}\{v_{AN} + v_{BN} + v_{CN}\} \tag{2}$$

The voltage vector can represent the three-phase voltage system:

$$v = \frac{2}{3}\{v_A + av_B + a^2 v_C\} \text{ with } a = e^{j\frac{2\pi}{3}} = -\frac{1}{2} + j\frac{\sqrt{3}}{2} \tag{3}$$

Therefore:

$$v = \frac{2}{3}\left[v_A - \frac{1}{2}(v_B + v_C) + j.\frac{\sqrt{3}}{2}(v_B - v_C)\right] = v_A + j.\frac{1}{\sqrt{3}}(v_B - v_C) \tag{4}$$

Representing voltage vector in $\alpha\beta$ coordinate: $v = v_\alpha + jv_\beta$
Where:

$$\begin{cases} v_\alpha = v_A \\ v_\beta = \frac{1}{\sqrt{3}}(v_B - v_C) \end{cases} \tag{5}$$

The phase angle of the vector v is determined:

$$\theta = arctg \frac{v_\beta}{v_\alpha} \tag{6}$$

Converting the output voltage vector on the $\alpha\beta$ coordinate system to the gh coordinate system with two axes g, and h, creats an angle of 60^0, the g axis coincides with the α axis. The base unit vector of the gh coordinate system is (7):

$$\begin{bmatrix} g_e \\ h_e \end{bmatrix} = \begin{bmatrix} e^{j0} \\ e^{j\frac{\pi}{3}} \end{bmatrix} = \begin{bmatrix} 1 \\ \frac{1}{2} + j\frac{\sqrt{3}}{2} \end{bmatrix} \tag{7}$$

The linear transformation does not change the vectors, keeping the coordinate origin, so a vector represented on two coordinate systems remains the same:

$$v = v_\alpha + jv_\beta = v_g g_e + v_h h_e \tag{8}$$

From (7) and (8):

$$v_\alpha + jv_\beta = v_g + v_h \left(\frac{1}{2} + j\frac{\sqrt{3}}{2} \right) \tag{9}$$

From (9), calculating easily:

$$\begin{cases} v_\alpha = v_g + \frac{1}{2}v_h \\ v_\beta = \frac{\sqrt{3}}{2}v_h \end{cases} \text{ or } \begin{cases} v_g = v_\alpha - \frac{1}{\sqrt{3}}v_\beta \\ v_h = \frac{2}{\sqrt{3}}v_\beta \end{cases} \tag{10}$$

Replacing (6) into (10):

$$\begin{cases} v_g = v_\alpha - \frac{1}{\sqrt{3}}v_\beta = v_A - \frac{1}{3}(v_B - v_C) = \frac{2}{3}(v_A - v_B) \\ v_h = \frac{2}{\sqrt{3}}v_\beta = \frac{2}{3}(v_B - v_C) \end{cases} \tag{11}$$

From (1) and (2):

$$\begin{cases} v_A - v_B = v_{AN} - v_{BN} = V_{DC}(k_A - k_B) \\ v_B - v_C = v_{BN} - v_{CN} = V_{DC}(k_B - k_C) \end{cases} \tag{12}$$

Therefore:

$$\begin{cases} v_g = \frac{2}{3}V_{DC}(k_A - k_B) \\ v_h = \frac{2}{3}V_{DC}(k_B - k_C) \end{cases} \text{ or } \begin{cases} v_g = \frac{2}{3}V_{DC}k_g \\ v_h = \frac{2}{3}V_{DC}k_h \end{cases} \tag{13}$$

Where:

$$\begin{cases} k_g = k_A - k_B \\ k_h = k_B - k_C \end{cases} \tag{14}$$

Seven-level H-bridge inverter in three phases, $k_A, k_B, k_C \in \{-3, -2, -1, 0, 1, 2, 3\}$. From (15) We can calculate the k_g, k_h coordinates of the vectors on the gh axis corresponding to the positions of the standard vector states V_i, and calculate the neutral voltage V_{ZN} from (2). spatial vector representation on the gh coordinate axis for a CHB three-phase inverter, 127 standard vectors are the vertices of the sub-triangles, with the numbering of the vectors increasing counterclockwise, from inside to outside.

If choosing $k_A = k$, where k must satisfy: $-\frac{M-1}{2} \leq k \leq \frac{M-1}{2}$, M is the number of levels of the multi-level inverter. From (15) for each vector state, the number of combinations of state levels obtained on the coordinate (a, b, c) is:

$$\begin{bmatrix} k_g \\ k_h \end{bmatrix} \Rightarrow \begin{bmatrix} k_A \\ k_B \\ k_C \end{bmatrix} = \begin{bmatrix} k \\ k - k_g \\ k - k_g - k_h \end{bmatrix} \text{ with } \begin{cases} -\frac{M-1}{2} \leq k \leq \frac{M-1}{2} \\ -\frac{M-1}{2} \leq k - k_g \leq \frac{M-1}{2} \\ -\frac{M-1}{2} \leq k - k_g - k_h \leq \frac{M-1}{2} \end{cases} \tag{15}$$

That is, k must satisfy:

$$\begin{cases} k \geq max\left\{-\frac{M-1}{2}, -\frac{M-1}{2} + k_g, -\frac{M-1}{2} + k_g + k_h\right\} \\ k \leq min\left\{\frac{M-1}{2}, \frac{M-1}{2} + k_g, \frac{M-1}{2} + k_g + k_h\right\} \end{cases} \quad (16)$$

it is possible to calculate all the combinations of state vectors for the hexagonal angles I, II, III, IV, V, VI if the number of voltage levels M, k_g, k are determined.

Step 2: synthesizing the output voltage vector from the standard state vector. Determining the position of the vector V in the large sector. The calculation becomes more straightforward if the symmetry of the space vector system in each of the sixths is used. Show on the vector plane three hexagonal coordinate systems (Z_{1x}, Z_{1y}), (Z_{2x}, Z_{2y}), (Z_{3x}, Z_{3y}) in Figure 4.
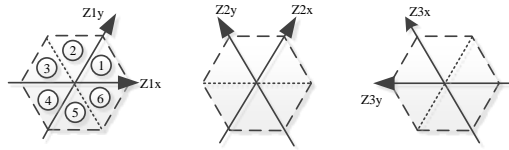

Figure 4. The coordinate systems of (Z_{1x}, Z_{1y}), (Z_{2x}, Z_{2y}), (Z_{3x}, Z_{3y})

The output voltage vector will be in one of the six sixths. First, we need to determine the projection of the vector $v^* = [v_\alpha^* + v_\beta^*]^T$ onto the two boundary vectors of the sixth angle by projecting the coordinates α, β onto the respective coordinate system (Z_{1x}, Z_{1y}), (Z_{2x}, Z_{2y}), (Z_{3x}, Z_{3y}).

$$\begin{cases} z_{1x} = v_\alpha - \frac{1}{\sqrt{3}}v_\beta \\ z_{1y} = \frac{2}{\sqrt{3}}v_\beta \end{cases} ; \begin{cases} z_{2x} = v_\alpha + \frac{1}{\sqrt{3}}v_\beta \\ z_{2y} = -v_\alpha + \frac{1}{\sqrt{3}}v_\beta \end{cases} ; \begin{cases} z_{3x} = \frac{2}{\sqrt{3}}v_\beta \\ z_{3y} = -v_\alpha - \frac{1}{\sqrt{3}}v_\beta \end{cases} \quad (17)$$

After determining the Z_{ij} coordinates, the algorithm tolocate the sector is shown in Figure 5. Locating the vector in the triangles formed by the three vertices as the normal vector. Representing the standard vector states on gh coordinates, the vectors will form equilateral triangles of length 1, with a 7-level three-phase inverter having 16 triangles in each sector. The triangle number in each sector will be numbered in anti-clockwise and inside-out order indicated Figure 6.
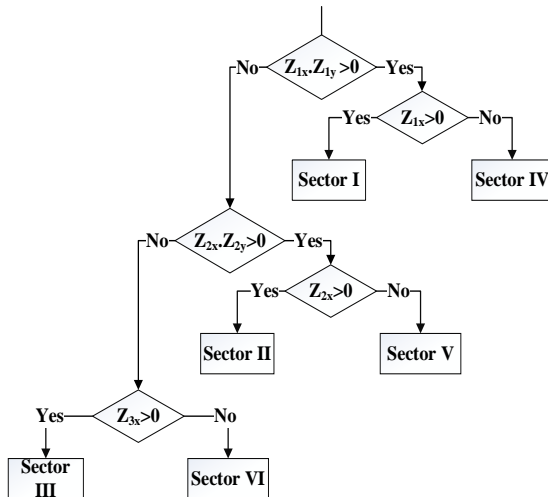

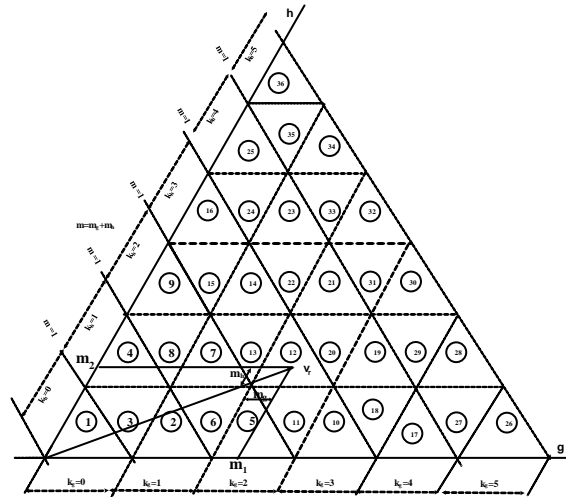Figure 5. Algorithm to determine large sector

Figure 6. Order of triangles in a large sector

Determine the two coefficients m_1 and m_2, which represent the ratio of the projection of the desired output voltage vector onto the two boundary vectors of the sixth angle:

$$\begin{cases} m_1 = \dfrac{z_{ix}}{(2/3)U_{DC}} \\ m_2 = \dfrac{z_{iy}}{(2/3)U_{DC}} \end{cases} \tag{18}$$

Based on m_1, m_2 determines the vector position in each triangle in Figure 6. Synthesise the output voltage vector from the three nearest reference vectors (calculation of modulation factor) the desired output vector lies in any triangle synthesized from the nearest three vectors, which are the vertices of this triangle. This can ensure an excellent harmonic component for the output voltage waveform. The calculation of output voltage vectors is shown in Figure 7.
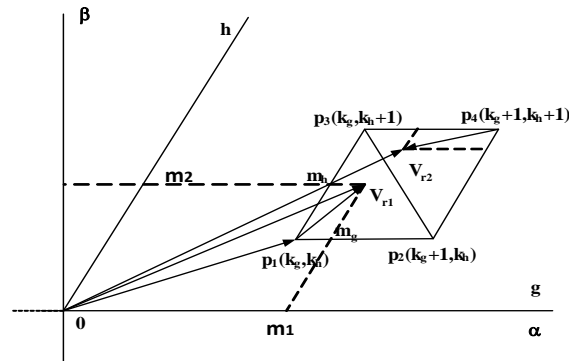

Figure 7. Summarizing the output voltage vector from the three vertex vectors of the triangle

Let m_g, m_h be the decimal parts apart from the integer part of the coordinates v_{ref} projected onto the Og, Oh axis respectively:

$$\begin{cases} m_g = v_{rg} - \lfloor |v_{rg}| \rfloor = v_{rg} - k_g \\ m_h = v_{rh} - \lfloor |v_{rh}| \rfloor = v_{rh} - k_h \end{cases} \tag{19}$$

V_{r1} can be synthesized from three vectors p_1, p_2, p_3 as (20):

$$V_{r1} = p_1 + m_g(p_2 - p_1) + m_h(p_3 - p_1) = (1 - m_g - m_h)p_1 + m_g p_2 + m_h p_3 \tag{20}$$

Similarly, V_{r2} can be synthesized from three vectors p_2, p_3, p_4:

$$\begin{aligned} V_{r2} &= p_4 + (1 - m_g)(p_3 - p_4) + (1 - m_h)(p_2 - p_4) \\ &= (m_g + m_h - 1)p_4 + (1 - m_g)p_3 + (1 - m_h)p_2 \end{aligned} \tag{21}$$

Step 3: the order of implementation of the optimal state vector in terms of the switches' switching times.

3.   SIMULATION RESULTS

Tables 2 and 3 show the simulation parameters. Conducting a simulation on MATLAB/Simulink for 5 s, the set speed gradually increases from 0 to the rated speed=592 (RMP) in the range of 0-1.5 s. It then gradually decreases, as shown in Figure 8, and the A phase voltage of the 7-level inverter is indicated in Figure 9. Controlling the motor speed levels based on the volume of people and traffic passing through the tunnel at different times of the day. During peak hours, the maximum rotation speed responds to the highest fan power, while at other times, the fan speed is controlled at lower speed levels.

Table 2. Parameters of the exhaust fan motor

Parameters	Symbol	Value	Parameters	Symbol	Value
Rated power	P_N	560 KW	Resistance of rotor	R_r	0.7217 Ω
Rated voltage	U_n	6 kV	Resistance of stator	R_s	0.7217 Ω
Power factor	cosφ	0.86	Rotor inductance	L_r	0.427 H
Rated speed	N_{dm}	592 rpm	Stator inductance	L_s	0.427H
Pole pair	p	10	Mutual inductance	L_m	0.4129 H
Rated current	I_n	91.636 A	Moment of inertia	J	32.8 kg.m^2
Rated torque	M_{rated}	9033 Nm			

Table 3. Parameters of 7-level inverter

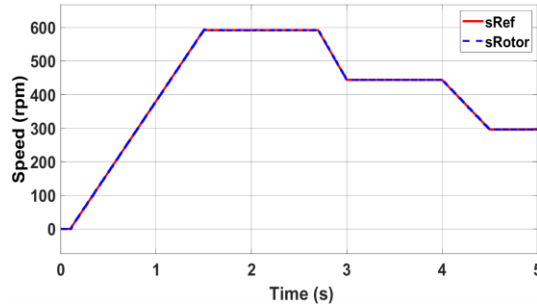| Parameters	Symbol	Value
DC-link voltage	V_{dc}	1700 V
DC side internal resistance per cell	R_{cell}	0.01 Ω
Capacitance per cell	C_{cell}	2500 μF
Carrier frequency	f	50 Hz
PWM pulse output frequency	f_{PWM}	2000 Hz

Figure 8. The speed response of induction motor
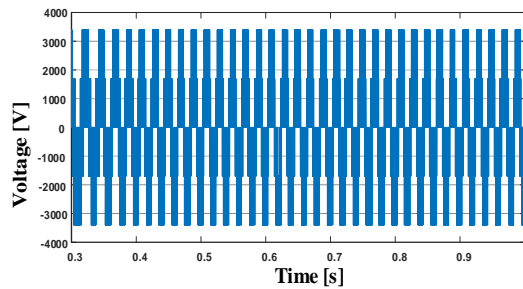
Figure 9. The a phase voltage of 7-level inverter

The total harmonic distortion (THD) of the load current, the voltage of the 7-level inverter with that of the 3-level one is demonstrated from Figures 10 to 13: the THD of the 7-level voltage is 2.55%, whereas the 3-level is 4.44%, the THD of the 7-level current is 0.42%, and the 3-level is 4.38%, which shows outstanding advantages of the 7-level inverter.
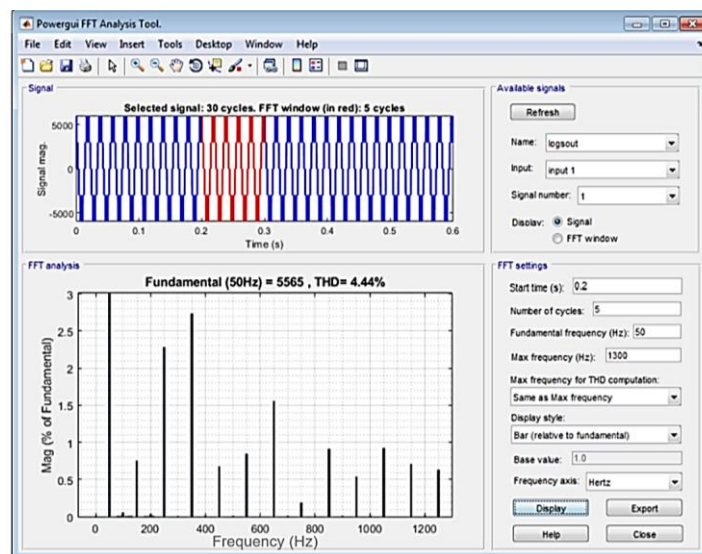

Figure 10. THD of phase a load voltage of 7-level inverter, 2.55%
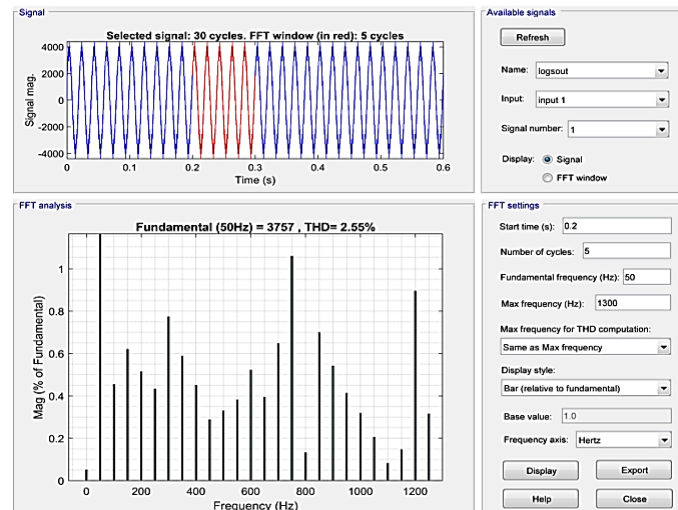
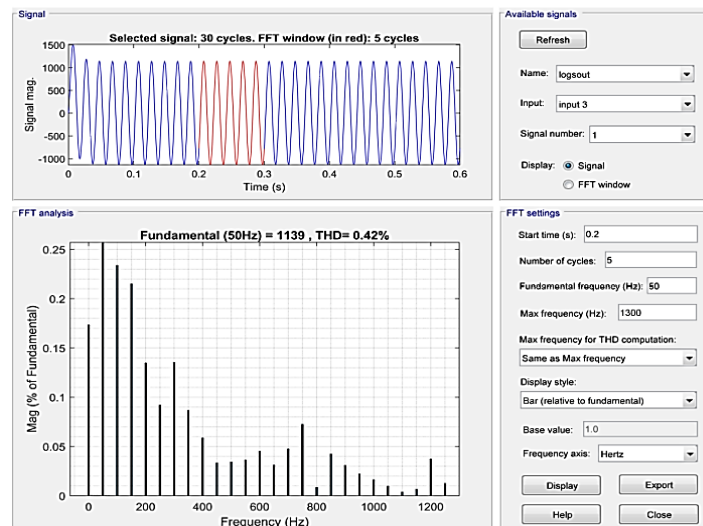Figure 11. THD of phase a load voltage of 3-level inverter, 4.44%

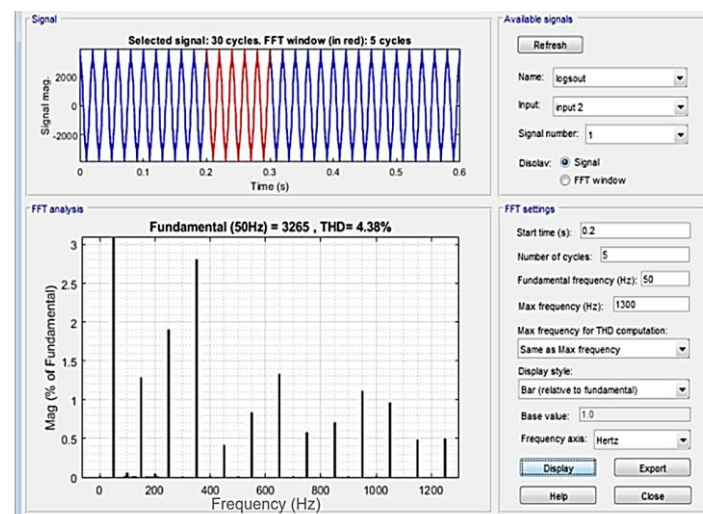Figure 12. THD of phase a load current of 7-level inverter, 0.42%

Figure 13. THD of phase a load current of 3-level inverter, 4.38%

4. CONCLUSION

Road tunnel ventilation systems play a crucial role in bringing fresh air into the tunnel and expelling polluted air, ensuring the safety of people inside tunnels. However, the exhaust fan's motor's large capacity and high voltage can cause significant harmonic distortion of the load current and the voltage. Therefore, the authors have proposed a 7-level inverter to control the exhaust fan motor. The simulation results in the article have shown the outstanding advantages of the CHB 7-level inverter to control the exhaust fan drive system in the Thu Thiem road tunnel; namely, comparison results of THD responses of phase A load current and voltage when using 7-level inverter are better than 3-level inverter (THD of the voltage of 7-level is 2.55%, and the 3-level is 4.44%; THD of the current of 7-level is 0.42%, and 3-level is 4.38%). Furthermore, the article also proposes a solution for operating the exhaust fan at appropriate speed levels according to the traffic density in the tunnel.

REFERENCES

[1] L. Sitao, L. Zhiqiang, L. Peifeng, J. Haifeng, and B. Linglin, "The analysis and discussion on ventilation and energy-saving of the tunnels of Long Highway," *IOP Conference Series: Earth and Environmental Science*, vol. 831, no. 1, p. 012029, Aug. 2021, doi: 10.1088/1755-1315/831/1/012029.

[2] F. Tarada, "Design, testing and application of an energy-efficient longitudinal ventilation system," *BHR Group - 14th International Symposium on Aerodynamics and Ventilation of Tunnels*, pp. 103–113, 2011.

[3] C. Guo, J. Xu, L. Yang, X. Guo, Y. Zhang, and M. Wang, "Energy-saving network ventilation technology of extra-long tunnel in climate separation zone," *Applied Sciences (Switzerland)*, vol. 7, no. 5, pp. 454–474, Apr. 2017, doi: 10.3390/app7050454.

[4] C. Guo, M. Wang, L. Yang, Z. Sun, Y. Zhang, and J. Xu, "A review of energy consumption and saving in extra-long tunnel operation ventilation in China," *Renewable and Sustainable Energy Reviews*, vol. 53, pp. 1558–1569, Jan. 2016, doi: 10.1016/j.rser.2015.09.094.

[5] M. Diaz *et al.*, "An overview of applications of the modular multilevel matrix converter," *Energies*, vol. 13, no. 21, pp. 5546–5583, Oct. 2020, doi: 10.3390/en13215546.

[6] M. Malinowski, K. Gopakumar, J. Rodriguez, and M. A. Perez, "A survey on cascaded multilevel inverters," *IEEE Transactions on Industrial Electronics*, vol. 57, no. 7, pp. 2197–2206, 2010, doi: 10.1109/TIE.2009.2030767.

[7] S. Sreelakshmi, M. S. Sujatha, J. R. Rahul, and T. Sutikno, "Reduced switched seven level multilevel inverter by modified carrier for high voltage industrial applications," *International Journal of Power Electronics and Drive Systems*, vol. 14, no. 2, pp. 872–881, 2023, doi: 10.11591/ijpeds.v14.i2.pp872-881.

[8] V. Govindaraj, S. Mayakrishnan, S. Venkatarajan, R. Raman, and R. Sundar, "Design and development of photovoltaic solar system based single phase seven level inverter," *Bulletin of Electrical Engineering and Informatics*, vol. 13, no. 1, pp. 58–66, Feb. 2024, doi: 10.11591/eei.v13i1.5168.

[9] Z. E. Abdulhamed, A. H. Esuri, and N. A. Abodhir, "New Topology of Asymmetrical Nine-Level Cascaded Hybrid Bridge Multilevel Inverter," in *2021 IEEE 1st International Maghreb Meeting of the Conference on Sciences and Techniques of Automatic Control and Computer Engineering, MI-STA 2021 - Proceedings*, IEEE, May 2021, pp. 430–434, doi: 10.1109/MI-STA52233.2021.9464511.

[10] J. Rodríguez, S. Bernet, B. Wu, J. O. Pontt, and S. Kouro, "Multilevel voltage-source-converter topologies for industrial medium-voltage drives," *IEEE Transactions on Industrial Electronics*, vol. 54, no. 6, pp. 2930–2945, Dec. 2007, doi: 10.1109/TIE.2007.907044.

[11] M. Arasteh, A. Rahmati, A. Abrishamifar, and S. Farhangi, "DTC on multilevel inverters for pumping and ventilation applications," in *2009 4th IEEE Conference on Industrial Electronics and Applications, ICIEA 2009*, IEEE, May 2009, pp. 2316–2320, doi: 10.1109/ICIEA.2009.5138612.

[12] A. K. Yarlagadda, V. K. Eate, Y. S. K. Babu, and A. Chakraborti, "A Modified Seven Level Cascaded H Bridge Inverter," *2018 5th IEEE Uttar Pradesh Section International Conference on Electrical, Electronics and Computer Engineering, UPCON 2018*, 2018, doi: 10.1109/UPCON.2018.8597096.

[13] S. Fan, Y. Yu, Y. Zhang, and H. Yang, "Multi-mode Synchronized PWM Schemes for three-level NPC Inverter," in *2019 22nd International Conference on Electrical Machines and Systems, ICEMS 2019*, IEEE, Aug. 2019, pp. 1–5, doi: 10.1109/ICEMS.2019.8921689.

[14] A. K. Sadigh, V. Dargahi, M. Abarzadeh, and S. Dargahi, "Reduced DC voltage source flying capacitor multicell multilevel inverter: analysis and implementation," *IET Power Electronics*, vol. 7, no. 2, pp. 439–450, Feb. 2014, doi: 10.1049/iet-pel.2013.0071.

[15] S. S. Barah and S. Behera, "An Optimize Configuration of H-Bridge Multilevel Inverter," in *ICPEE 2021 - 2021 1st International Conference on Power Electronics and Energy*, IEEE, Jan. 2021, pp. 1–4, doi: 10.1109/ICPEE50452.2021.9358533.

[16] G. Singh and V. K. Garg, "THD analysis of cascaded H-bridge multi-level inverter," in *4th IEEE International Conference on Signal Processing, Computing and Control, ISPCC 2017*, IEEE, Sep. 2017, pp. 229–234, doi: 10.1109/ISPCC.2017.8269680.

[17] J. Ebrahimi, E. Babaei, and G. B. Gharehpetian, "A new multilevel converter topology with reduced number of power electronic components," *IEEE Transactions on Industrial Electronics*, vol. 59, no. 2, pp. 655–667, Feb. 2012, doi: 10.1109/TIE.2011.2151813.

[18] P. Panagis, F. Stergiopoulos, P. Marabeas, and S. Manias, "Comparison of state of the art multilevel inverters," in *PESC Record - IEEE Annual Power Electronics Specialists Conference*, IEEE, Jun. 2008, pp. 4296–4301, doi: 10.1109/PESC.2008.4592633.

[19] S. N. Rao, D. V. A. Kumar, and C. S. Babu, "New multilevel inverter topology with reduced number of switches using advanced modulation strategies," *Proceedings of 2013 International Conference on Power, Energy and Control, ICPEC 2013*, 2013, pp.

693–699, doi: 10.1109/ICPEC.2013.6527745.

[20] R. A. Krishna and L. P. Suresh, "A brief review on multi level inverter topologies," in *Proceedings of IEEE International Conference on Circuit, Power and Computing Technologies, ICCPCT 2016*, IEEE, Mar. 2016, pp. 1–6, doi: 10.1109/ICCPCT.2016.7530373.

[21] V. T. Ha, T. T. Minh, N. T. Lam, and N. H. Quang, "Experiment based comparative analysis of stator current controllers using predictive current control and proportional integral control for induction motors," *Bulletin of Electrical Engineering and Informatics*, vol. 9, no. 4, pp. 1662–1669, Aug. 2020, doi: 10.11591/eei.v9i4.2084.

[22] T. D. Do, N. D. Le, V. H. Phuong, and N. T. Lam, "Implementation of FOC algorithm using FPGA for GaN-based three phase induction motor drive," *Bulletin of Electrical Engineering and Informatics*, vol. 11, no. 2, pp. 636–645, Apr. 2022, doi: 10.11591/eei.v11i2.3569.

[23] R. Shriwastava *et al.*, "Performance analysis of FOC space vector modulation DCMLI driven PMSM drive," *Bulletin of Electrical Engineering and Informatics*, vol. 12, no. 5, pp. 2682–2692, Oct. 2023, doi: 10.11591/eei.v12i5.4554.

[24] S. K. Chien *et al.*, "Enhanced DTC induction motor drives for THD minimization performance improvement with multilevel inverter," *International Journal of Power Electronics and Drive Systems*, vol. 13, no. 1, pp. 93–101, 2022, doi: 10.11591/ijpeds.v13.i1.pp93-101.

[25] S. Farzana, Y. Sumith, and K. Ravisankar, "Performance enhancement of three phase induction motor by using multi level inverter," in *IEEE International Conference on Innovative Mechanisms for Industry Applications, ICIMIA 2017 - Proceedings*, IEEE, Feb. 2017, pp. 720–725, doi: 10.1109/ICIMIA.2017.7975559.

BIOGRAPHIES OF AUTHORS

An Thi Hoai Thu Anh 🔘 📧 sc ⦿ received her Engineer (1997), M.Sc. (2002) degrees in Industrial Automation Engineering from Hanoi University of Science and Technology, and completed Ph.D. degree in 2020 from University of Transport and Communications (UTC). Now, she is a lecturer at the Faculty of Electrical and Electronic Engineering at the University of Transport and Communications (UTC). Her current interests include power electronic converters, electric motor drive, and saving energy solutions applied for industry and transportation. She can be contacted at email: htanh.ktd@utc.edu.vn.

Tran Hung Cuong 🔘 📧 sc ⦿ received his Engineer (2010), M.Sc. (2013) degrees in Industrial Automation Engineering from Hanoi University of Science and Technology, and completed Ph.D. degree in 2020 from Hanoi University of Science (HUST). Now, he is a lecturer of Faculty of Electrical and Electronic Engineering under ThuyLoi University s (TLU). His current interests include power electronic converters, electric motor drive, convert electricity from renewable energy sources to the grid, and saving energy solutions applied for grid and transportation. He can be contacted at email: cuongth@tlu.edu.vn.

Tran Van Khoi 🔘 📧 sc ⦿ received B.S. and M.S. degree in Electrical Engineering and Automation from the University of Transport and Communications, Hanoi, Vietnam in 2004 and 2009, respectively, and received Ph.D. degree from Beijing Jiaotong University, Beijing, China in 2019. He is currently a lecturer of Electrical and Electronic Faculty in University of Transport and Communications (UTC). His research interests are optimal techniques and energy management strategies. He can be contacted at email: tvkhoi.ktd@utc.edu.vn.